Progress of Theoretical Physics, Vol. 104, No. 2, August 2000

Endpoint of the Electroweak Phase Transition Using the Auxiliary Mass Method

Kenzo OGURE*) and Joe SATO*,**)

Institute for Cosmic Ray Research, University of Tokyo, Tanashi 188-8502, Japan
**Research Center for Higher Education, Kyushu University, Ropponmatsu Fukuoka 810-8560, Japan*

(Received December 8, 1999)

We study the endpoint of the electroweak phase transition using the auxiliary mass method. The endpoint is $m_H \sim 40$ GeV in the case $m_t = 0$ GeV and strongly depends on the top quark mass. The first-order phase transition disappears at $m_t \sim 160$ GeV. The renormalization effect of the top quark is significant.

The electroweak phase transition is one of the most important phase transitions in the early universe, since it may account for the baryon number of the present universe.[1] This phase transition was first investigated using the perturbation theory of finite-temperature field theory. In this theory, a first-order phase transition is predicted with an effective potential.[2),3)] The perturbation theory, however, has a difficulty due to an infrared divergence caused by light bosons and cannot give reliable results in the case that the Higgs boson mass m_H is comparable to or greater than the weak boson mass. For this reason, lattice Monte Carlo simulations represent the most powerful method at present and are still used to investigate details of the phase transition.[4)-8)] According to their results, the electroweak phase transition is of first order if m_H is less than an endpoint $m_{H,c} \sim 70$ GeV. It becomes second order just at the endpoint. Beyond the endpoint, we have no phase transition. This implies that no observable quantities have discontinuities. As far as we know, three other non-perturbative methods predict the existence of the endpoint.[9)-11)] The endpoint is found to be below 100 GeV by all three of these methods.

The auxiliary-mass method is a new method to avoid the infrared divergence at a finite temperature T.[12)-15)] This method is based on a simple idea as follows. We first add a large auxiliary mass to light bosons, which cause the infrared divergence, and calculate an effective potential at the finite temperature. Due to the auxiliary mass, the effective potential is reliable at any temperature. We next extrapolate this effective potential to the true mass by integrating an evolution equation. This is carried out below. We applied this method to the Z_2-invariant scalar model and the $O(N)$-invariant scalar model and obtained satisfactory results.[13)-15)]

We apply the method to the Standard Model and investigate the electroweak phase transition in the present paper. We add an auxiliary mass $M \gtrsim T$ only to the Higgs boson, which becomes very light owing to a cancellation between its negative

*) E-mail: ogure@octopus.phys.sci.kobe-u.ac.jp
**) E-mail: joe@rc.kyushu-u.ac.jp

tree mass and positive thermal mass for small field expectation values around the critical temperature. We note that the infrared divergence from the Higgs boson is always serious if the phase transition is second order or weakly first order.[3] In the Standard Model, transverse modes of the gauge fields also have small masses at small field expectation values, since they do not have thermal mass at one loop order. We give discussion summarizing the influence of these modes.

An effective potential is calculated as follows in the Landau gauge:[2),3)]

$$\begin{aligned} V(M^2) = {} & \frac{M^2}{2}\phi^2 + \frac{\lambda}{4!}\phi^4 + f_{BT}(m_H^2(\phi)) + 3f_{BT}(m_{NG}^2(\phi)) \\ & +4f_{BT}(M_W^2(\phi)) + 4f_{G0}(M_W^2(\phi)) \\ & +2f_{BT}(M_{WL}^2(\phi)) + 2f_{G0}(M_{WL}^2(\phi)) \\ & +2f_{BT}(M_Z^2(\phi)) + 2f_{G0}(M_Z^2(\phi)) \\ & +f_{BT}(M_{ZL}^2(\phi)) + f_{G0}(M_{ZL}^2(\phi)) \\ & +f_{BT}(M_{\gamma L}^2(\phi)) + f_{G0}(M_{\gamma L}^2(\phi)) \\ & +12f_{FT}(m_t^2(\phi)) + 12f_{F0}(m_t^2(\phi)). \end{aligned} \tag{1}$$

Here,

$$\begin{aligned} m_H^2(\phi) &= M^2 + \frac{\lambda}{2}\phi^2, \quad m_{NG}^2(\phi) = M^2 + \frac{\lambda}{6}\phi^2, \\ M_W^2(\phi) &= \frac{g_2^2\phi^2}{4}, \quad M_{WL}^2(\phi) = \frac{g_2^2\phi^2}{4} + \frac{11g_2^2T^2}{6}, \\ M_Z^2(\phi) &= \frac{(g_2^2+g_1^2)\phi^2}{4}, \quad m_t(\phi) = \frac{g_Y^2\phi^2}{2}, \end{aligned}$$

$$\begin{pmatrix} M_{ZL}^2 & 0 \\ 0 & M_{\gamma L}^2 \end{pmatrix} = \boldsymbol{T}^\dagger \begin{pmatrix} \frac{g_2^2\phi^2}{4} + \frac{11g_2^2T^2}{6} & -\frac{g_1g_2\phi^2}{4} \\ -\frac{g_1g_2\phi^2}{4} & \frac{g_1^2\phi^2}{4} + \frac{11g_2^2T^2}{6} \end{pmatrix} \boldsymbol{T},$$

$$\begin{aligned} f_{BT}(m^2) &= \frac{T}{2\pi^2}\int_0^\infty dk\ k^2 \log\left\{1 - \exp\left(-\frac{\sqrt{k^2+m^2}}{T}\right)\right\}, \\ f_{FT}(m^2) &= \frac{T}{2\pi^2}\int_0^\infty dk\ k^2 \log\left\{1 + \exp\left(-\frac{\sqrt{k^2+m^2}}{T}\right)\right\}, \\ f_{G0}(m^2) &= \frac{m^4}{64\pi^2}\left\{\log\left(\frac{m^2}{\bar{\mu}^2}\right) - \frac{5}{6}\right\}, \\ f_{F0}(m^2) &= -\frac{m^4}{64\pi^2}\left\{\log\left(\frac{m^2}{\bar{\mu}^2}\right) - \frac{3}{2}\right\}. \end{aligned}$$

In the above equations, λ, g_2, g_1 and g_Y are coupling constants for the Higgs boson, $SU(2)$ gauge field, $U(1)$ gauge field, and top Yukawa, respectively. The matrix $\boldsymbol{T}$ is orthogonal and diagonalizes the mass matrix for the Z boson and photon at finite temperature. We renormalized the effective potential using the $\overline{MS}$ scheme with a

renormalization scale $\bar{\mu}$. A zero-temperature contribution from the Higgs boson is neglected because it is small in the mass region we consider. The ring diagrams are added only to the weak bosons and the Z-boson, since the Higgs bosons have large auxiliary mass and do not require resummation. We then extrapolate this effective potential at the auxiliary mass squared M^2 to that of the true mass squared $-\nu^2$ using an evolution equation. Since we add the auxiliary mass only to the Higgs boson, the evolution equation is the same as that for the $O(4)$-invariant scalar model, which was constructed in[*] Ref. 15):

$$\begin{aligned}\frac{\partial V}{\partial m^2} &= \frac{1}{2}\bar{\phi}^2 + \frac{1}{4\pi^2}\int_0^\infty dk \frac{k^2}{\sqrt{k^2+\frac{\partial^2 V}{\partial \bar{\phi}^2}}} \frac{1}{e^{\frac{1}{T}\sqrt{k^2+\frac{\partial^2 V}{\partial \bar{\phi}^2}}}-1} \\ &\quad + \frac{3}{4\pi^2}\int_0^\infty dk \frac{k^2}{\sqrt{k^2+\frac{1}{\bar{\phi}}\frac{\partial V}{\partial \bar{\phi}}}} \frac{1}{e^{\frac{1}{T}\sqrt{k^2+\frac{1}{\bar{\phi}}\frac{\partial V}{\partial \bar{\phi}}}}-1}. \end{aligned} \tag{2}$$

A non-perturbative effective potential free from infrared divergence can be obtained by solving the evolution equation (2) with the initial conditions given in Eq. (1) numerically.

Before giving our numerical results, we relate the parameters ν^2, λ, g_2, g_1 and g_Y to physical quantities at zero-temperature.[3] We have

$$\begin{aligned}\lambda &= \frac{3m_{H0}^2}{\phi_0^2} - \frac{3}{32\pi^2}\left[\frac{3}{2}g_2^4\left\{\log\left(\frac{M_{W0}^2}{\bar{\mu}^2}\right)+\frac{2}{3}\right\}\right. \\ &\quad + \frac{3}{4}\left(g_1^2+g_2^2\right)^2\left\{\log\left(\frac{M_{Z0}^2}{\bar{\mu}^2}\right)+\frac{2}{3}\right\} \\ &\quad \left. - 12g_Y^4\log\left(\frac{m_{t0}^2}{\bar{\mu}^2}\right)\right], \\ \nu^2 &= \frac{m_{H0}^2}{2} - \frac{\phi_0^2}{64\pi^2}\left\{\frac{3}{2}g_2^4+\frac{3}{4}(g_1^2+g_2^2)^2-12g_Y^4\right\}, \\ M_{W0}^2 &= \frac{g_2^2\phi_0^2}{4}, \quad M_{Z0}^2 = \frac{(g_2^2+g_1^2)\phi_0^2}{4}, \\ m_{t0}^2 &= \frac{g_Y^2\phi_0^2}{2}, \quad \phi_0 = 246 \text{ GeV}. \end{aligned} \tag{3}$$

Radiative corrections at the one-loop order are included in the equations for ν^2 and λ since they are large, especially in the case that the Higgs boson mass is small. The effective potential Eq. (1) does not depend on $\bar{\mu}$ using λ in Eq. (3) at this order. Below, we fix the masses of the weak bosons and the Z-boson as $M_{W0} = 80$ GeV and $M_{Z0} = 92$ GeV.

We first investigate a $SU(2) \times U(1)$ gauge-plus-Higgs theory, corresponding to the case $m_t = 0$. We give only the results obtained by setting $M = T$, since similar

[*] We neglected the momentum dependence of the full self-energy in Ref. 14). This corresponds to the local potential approximation of the systematic derivative expansion of the effective action.

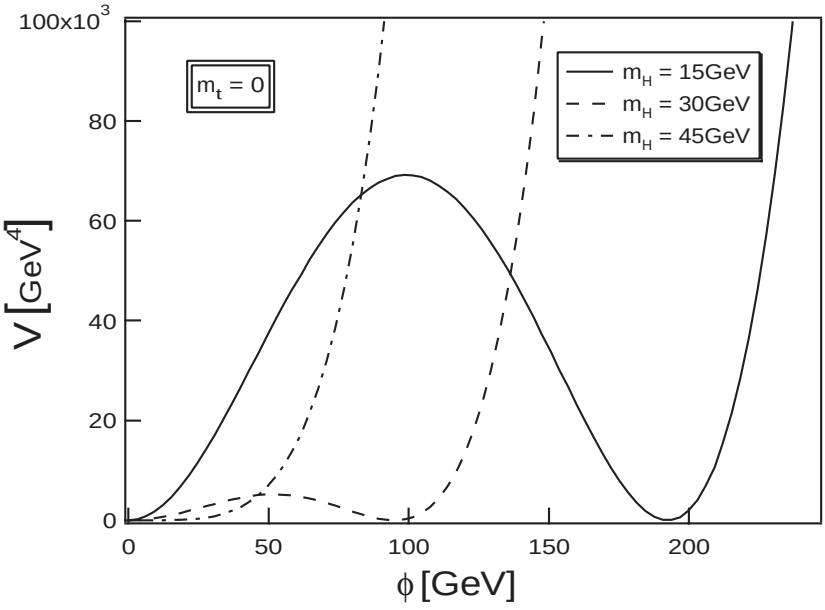

Fig. 1. The real parts of the effective potentials at the critical temperature for m_H =15, 30 and 45 GeV. The first-order phase transition becomes weaker for smaller values of the Higgs mass, and finally disappears.

results were obtained by setting $M = \frac{T}{2}$ and $M = 2T$, as in the case of Ref. 13). This is quite natural, since the restriction on M is $M \gtrsim T$. The real parts of the effective potentials at the critical temperature are shown in Fig. 1 for m_H =15, 30 and 45 GeV. The first order phase transition becomes weaker for smaller values of the Higgs mass, and finally disappears. The imaginary part of the effective potential, which represents the instability of the vacuum, as in Ref. 13), also exists for the range of ϕ, where the curvature of the real part of the effective potential is negative. We do not show this imaginary part, since it has nothing to do with our main focus, the existence of the endpoint. They are compared to effective potentials obtained using the ring resumed perturbation theory at the one-loop order without the high-temperature expansion in Fig. 2. We find clearly that they are similar for smaller values of m_H and different for larger values of m_H. This is consistent with the fact that the ring-resumed perturbation theory is reliable only for smaller values of the Higgs mass, i.e., for $m_H \ll M_W$.[3] We plot the ratio of the critical field expectation value to the critical temperature, ϕ_c/T_c, as a function of m_H in Fig. 3. This quantity indicates the strength of the first-order phase transition and is important in estimating the sphaleron rate, which plays a very important role in electroweak baryogenesis.[16),17)] The endpoint is determined as $m_{H,c} = 38$ GeV from Fig. 3. This figure also shows that the results obtained using the auxiliary mass method and the perturbation theory are similar for smaller values of m_H but differ for larger values, i.e., for $m_H \gtrsim 30$ GeV.

We next investigate more realistic cases in which the top quark mass is finite. The same ratios are displayed in Fig. 4 for various values of m_t. This figure shows

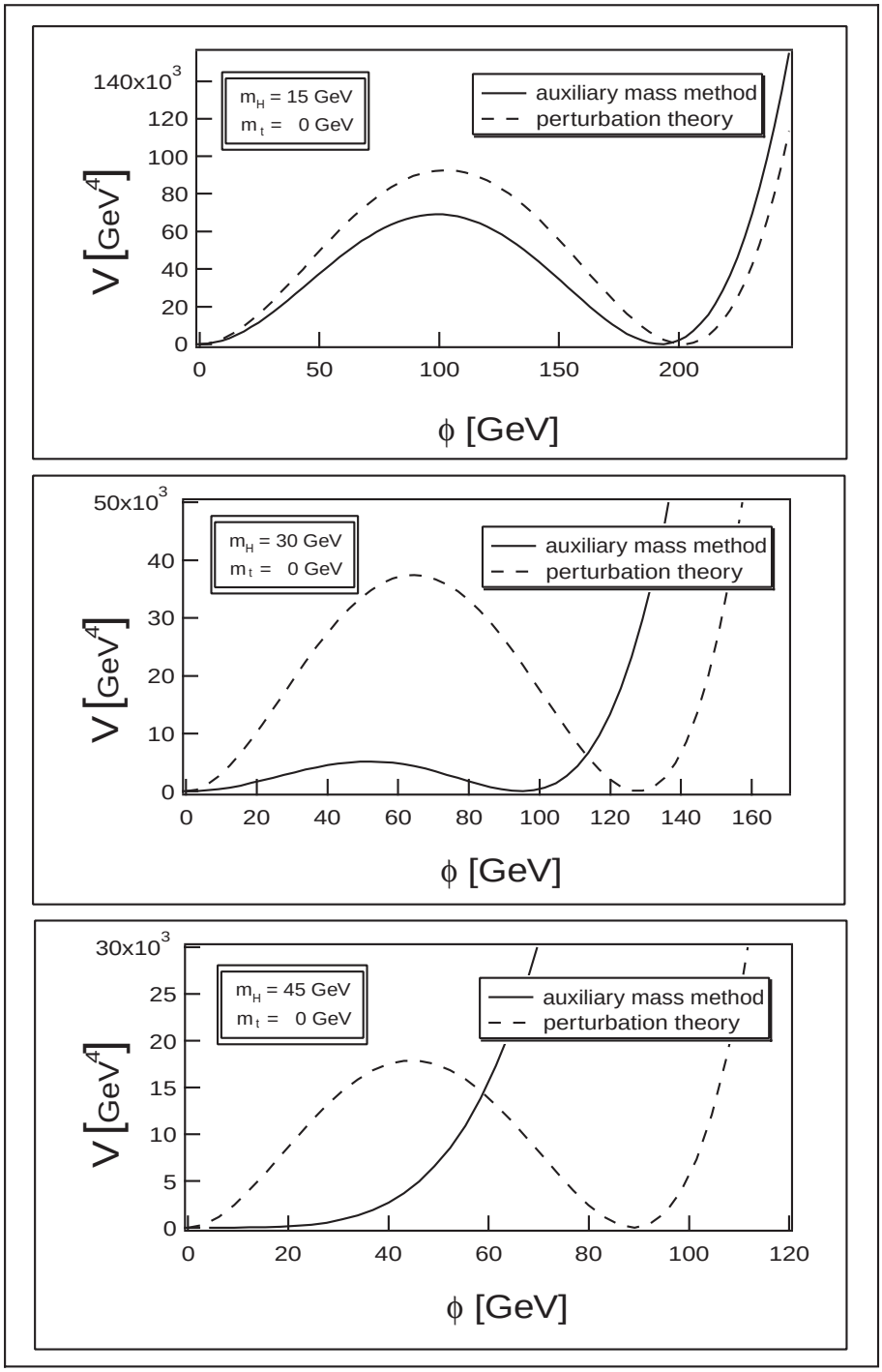

Fig. 2. The real parts of the effective potentials at the critical temperature obtained using the auxiliary mass method and the perturbation theory for m_H =15, 30 and 45 GeV. These results are similar for smaller values of m_H and different for larger values of m_H.

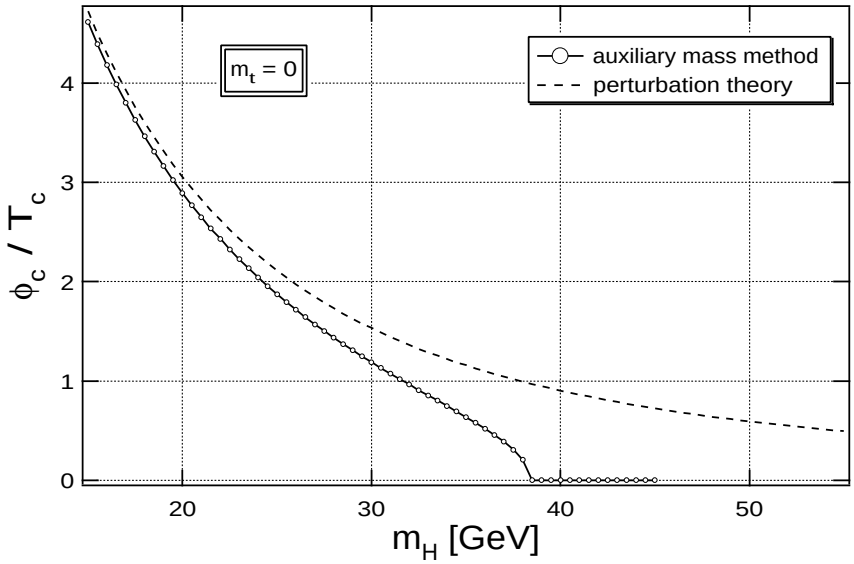

Fig. 3. The ratio of the critical field expectation value to the critical temperature, ϕ_c/T_c. The results obtained using the auxiliary mass method and the perturbation theory are similar for smaller values of m_H ($m_H < 30$ GeV) and different for larger values ($m_H > 30$ GeV.)

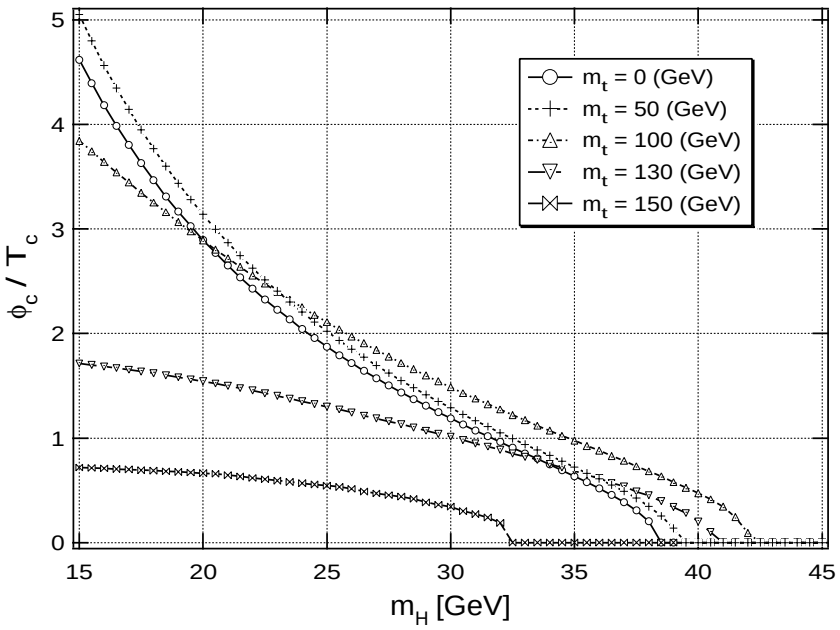

Fig. 4. The ratio of the critical-field expectation value to the critical temperature, ϕ_c/T_c. The phase transition is weaker for larger top quark mass.

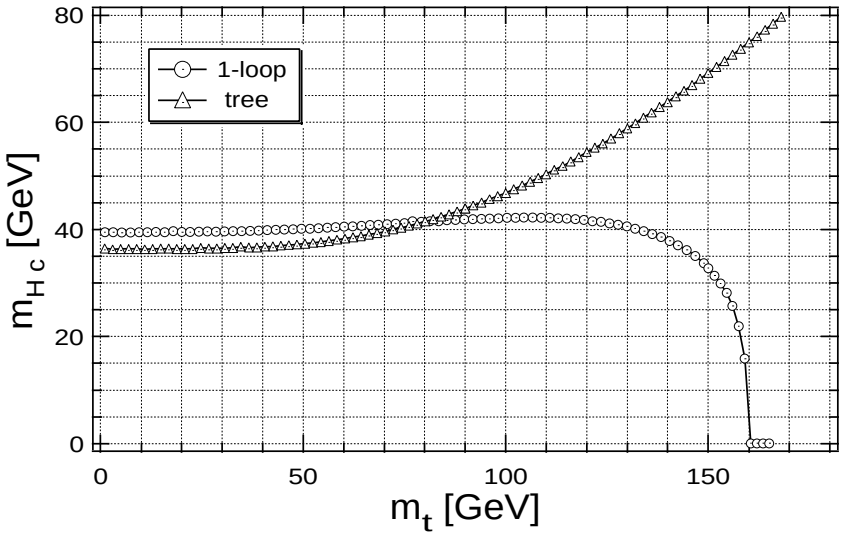

Fig. 5. The endpoint of the Higgs boson as a function of the top quark mass. The graph labeled "tree" was obtained using only the first terms in Eq. (3) for ν^2 and λ. This corresponds to matching the parameters with physical observable quantities at the tree level. The graph labeled "1-loop" was obtained using all terms in Eq. (3) for ν^2 and λ. This corresponds to matching the parameters with physical observable quantities at the one-loop level.

that the strengths of the first-order phase transition are almost the same for $m_t \lesssim 100$ GeV and become weaker for $m_t \gtrsim 100$ GeV rapidly. The endpoints are shown in Fig. 5 as functions of m_t. The graph labeled "1-loop" was obtained using Eqs. (1) and (3), which take into account the zero-temperature radiative corrections from the top quark and gauge fields. The contribution from the top quark is much larger than that from the gauge fields. On the other hand, the graph labeled "tree" was obtained without the zero-temperature radiative correction, omitting the contributions from f_{G0} and f_{F0} from Eq. (1) and leaving only the first terms of Eq. (3) for λ and ν^2. These graphs do not differ greatly for smaller values of the top quark mass, $m_t \lesssim 100$ GeV. Their behavior, however, differs drastically for larger values of the top quark mass, $m_t \gtrsim 100$ GeV. Surprisingly, the endpoint vanishes for $m_t \gtrsim 160$ GeV in the "1-loop" results, though it increases in the "tree" results. These results tell us that fermionic degrees of freedom play significant roles in the phase transition through the renormalization effects at zero temperature. We also conclude that there are no first-order phase transitions for $m_t = 175$ GeV, no matter how small the Higgs boson mass.

In the present paper, we have calculated the effective potentials of the Standard Model using the auxiliary mass method at finite temperature. We first investigated an $SU(2) \times U(1)$ gauge-plus-Higgs theory, corresponding to the case $m_t = 0$. The phase transition was found to be first order, and our results are similar to the results obtained using the perturbation theory for smaller values of m_H, i.e., $m_H \sim 15$ GeV. However, we found that the phase transition becomes weaker for larger values, $M_H \sim 30$ GeV and finally disappears, in contrast to the results from perturbation

theory. We found that the endpoint is at $m_{H,c} = 38$ GeV in this case. This is qualitatively consistent with the results of the Lattice Monte Carlo simulations [5)-8)] and other non-perturbative methods. [9)-11)] The value we obtained for the endpoint, however, is smaller than those obtained with these methods. We next investigated the more realistic case in which the top quark mass is finite. In this case, we found that the endpoint is strongly dependent on m_t and disappears for $m_t \gtrsim 160$ GeV. Also, the renormalization effects from the top quark are significant. Lattice Monte Carlo simulations, however, do not exhibit this behavior. [18)] We can think of two possible reasons for this: (1) Since our results differ from those of the lattice Monte Carlo simulation by factors of 2 in a $SU(2) \times U(1)$ gauge-plus-Higgs theory quantitatively (probably because of the higher loop effect of gauge fields and the approximation that we used in obtaining Eq. (2)), the same behavior may be found at a larger top quark mass in the lattice Monte Carlo simulation. (2) Since the one-loop correction to the *effective potential* at zero temperature is significant, the 3D effective theory, which has no fermionic degrees of freedom, may not reflect the effect appropriately.

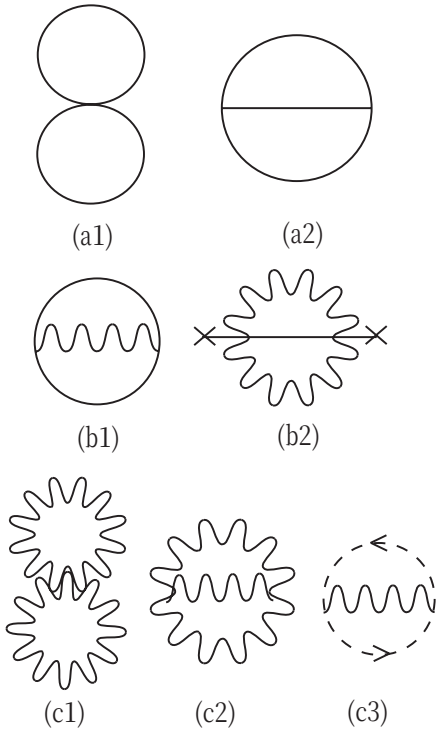

Fig. 6. Two-loop graphs with the Higgs boson and the gauge boson. (a) Graphs with only the Higgs boson. These have no infrared divergence, thanks to the auxiliary mass. (b) Graphs with the Higgs boson and the gauge field. Here, the infrared behavior is controlled by the auxiliary mass. (c) Graphs with only gauge boson. These have poor infrared behaviour.

We now discuss the higher-loop effect of gauge fields. Since we did not introduce the auxiliary mass into gauge fields, the loop expansion parameter for the gauge fields was not improved. We, therefore, controlled only the infrared divergence of graphs involving the Higgs boson field. In this sense, our method improves the infrared divergence partially. We thus consider a "hybrid" method to improve the approximation. In this method, we introduce the auxiliary mass for the Higgs boson and use a perturbative expansion for the gauge boson.*) As an illustrative example, we now explain how to evaluate the two-loop effect. Using the auxiliary mass method, we need not take into account Figs. 6(a1) and (a2), thanks to the auxiliary mass. In addition, we need not take into account Figs. 6(b1) and (b2), which have large infrared effect [$\propto \phi^2 T^2 \log(\phi)$] in the ordinary pertur-

*) Perturbative expansion for non-Abelian gauge fields cannot be calculated to arbitrary order, due to the infrared divergence. Our method cannot solve this problem.

bation theory, since the auxiliary mass controls the infrared effect [$\propto \phi^2 T^2 \log(M)$]. The only graphs we have to take into account are those in Figs. 6(c1), (c2) and (c3). We need not take into account as many graphs as in the ordinary perturbation theory because most graphs have good infrared behavior thanks to the auxiliary mass. We expect that this two-loop effect reduces the qualitative gap between our results and those of lattice simulations.*)

Finally, the strongly first-order phase transition necessary for the electroweak baryogenesis was not found in the Standard Model. We will apply this method to extensions of the Standard Model.

One of the authors (K.O.) is supported by JSPS.

References

1) V. Kuzmin, V. Rubakov and M. E. Shaposhnikov, Phys. Lett. **B155** (1985), 36.
2) M. E. Carrington, Phys. Rev. **D45** (1992), 2933.
3) P. Arnold and O. Espinosa, Phys. Rev. **D47** (1993), 3546.
4) K. Rummukainen, M. Tsypin, K. Kajantie, M. Laine and M. E. Shaposhniko, Nucl. Phys. **B532** (1998), 283 (references therein).
5) F. Csikor, Z. Fodor and J. Heitger, Phys. Rev. Lett. **82** (1999), 21 (references therein).
6) E.- M. Ilgenfritz, A. Schiller and C. Strecha, Eur. Phys. J. **C8** (1999), 135 (references therein).
7) F. Karch, T. Neuhaus, A. Patós and J. Rank, Nucl. Phys. **474** (1996), 217.
8) Y. Aoki, F. Csikor, Z. Fodor and A. Ukawa, hep-lat/9901021.
9) W. Buchmuller and O. Philipsen, Phys. Lett. **B354** (1995), 403.
10) N. Tetradis, Phys. Lett. **B409** (1997), 355.
11) S. J. Huber, A. Laser, M. Reuter and M. G. Schmidt, Nucl. Phys. **B539** (1999), 477.
12) I. T. Drummond, R. R. Horgan, P. V. Landshoff and A. Rebhan, Phys. Lett. **B398** (1997), 326.
13) T. Inagaki, K. Ogure and J. Sato, Prog. Theor. Phys. **99** (1998), 119.
14) K. Ogure and J. Sato, Phys. Rev. **D57** (1998), 7460.
15) K. Ogure and J. Sato, Phys. Rev. **D58** (1998), 085010.
16) M. S. Manton, Phys. Rev. **D28** (1983), 2019.
17) F. R. Kllinkhamer and M. S. Manton, Phys. Rev. **D30** (1984), 2212.
18) K. Kajantie, M. Laine, K. Rummukainen and M. E. Shaposhniko, Nucl. Phys. **B466** (1996), 189.

*) Investigation of the two-loop effect is under way.